ELSEVIER

Marine Geology 231 (2006) 163 – 180

MARINE GEOLOGY
INTERNATIONAL JOURNAL OF MARINE GEOLOGY, GEOCHEMISTRY AND GEOPHYSICS

www.elsevier.com/locate/margeo

Submarine hydrothermal activity and mineralization on the Kurile and western Aleutian island arcs, N.W. Pacific

G.P. Glasby [a,*], G.A. Cherkashov [a], G.M. Gavrilenko [b], V.A. Rashidov [c], I.B. Slovtsov [a]

[a] *VNII Oceangeologia, 1, Angliysky Pr., 190121 St. Petersburg, Russia*
[b] *Institute of Volcanology, Far East Division, Russian Academy of Sciences, 9, Piip Blvd, Petropavlosk-Kamchatky, Russia*
[c] *Institute of Volcanic Geology and Geochemistry, Far East Division, Russian Academy of Sciences, 9, Piip Blvd, Petropavlosk-Kamchatky, Russia*

Received 26 November 2005; received in revised form 4 May 2006; accepted 6 June 2006

Abstract

The Kurile Arc consists of at least 100 submarine volcanoes and 5 submarine caldera located mainly in the rear arc. The arc is seismically very active, particularly in the south, and is characterized by extensive volcanism and hydrothermal activity. At least one subaerial volcano on the arc (Medvezhy located on Iturup island) has an extremely shallow magma chamber and is intensely active. Three types of submarine hydrothermal deposit were recovered from this area, hydrothermal manganese crusts, nontronite and hydrothermal manganese crusts overlain by hydrogenous manganese oxides. In addition, submarine hydrothermal Fe oxyhydroxides enriched in P were sampled from the submerged caldera of Kraternaya Bight in the central part of the arc. These deposits appear to be analagous to deposits from Santorini caldera on the Aegean Arc. Piip submarine volcano located in the western Aleutian Arc is characterized by two shallow summit craters. Both intermediate-temperature (anhydrite, gypsum, barite, amorphous silica, pyrite, calcite and aragonite) and low-temperature (nontronite, Fe oxyhydroxides, hisingerite and ferromanganese crusts) hydrothermal minerals were recovered from this seamount together with bacterial mats and giant clams. The maximum measured temperature of the hydrothermal fluids was 133 °C, although the actual temperature may have reached 250 °C. Both the Kurile and Aleutian Arcs have the potential to host major submarine hydrothermal systems. Detailed exploration of these poorly studied areas using modern geophysical, geochemical and sampling techniques is therefore strongly recommended.

Keywords: Kuriles arc; Aleutian arc; submarine hydrothermal mineralization; Kraternaya bight; Piip volcano

1. Introduction

Over the past decade, knowledge of submarine hydrothermal systems and the accompanying submarine hydrothermal mineralization at convergent plate margins of the western Pacific has increased enormously. Particular interest has focussed on the Okinawa Trough (Glasby and Notsu, 2003), the Izu-Bonin Arc (Iizasa et al., 1999, 2004; Glasby et al., 2000; Fiske et al., 2001), the Mariana Arc (Embley et al., 2004) and the Tonga–Kermadec Arc (de Ronde et al., 2001, 2003a,b; Wright et al., 2001; Baker et al., 2004; Massoth et al., 2004). However, there has been

* Corresponding author. c/o Professor G. Wörner, Abt. Geochemie, GZG, Univeriität Göttingen, Goldschmidtstr. 1, D-37077 Universität Göttingen, Germany.
E-mail address: g.p.glasby@talk21.com (G.P. Glasby).

0025-3227/$ - see front matter
doi:10.1016/j.margeo.2006.06.003

no corresponding increase in knowledge of submarine hydrothermal systems in the Kurile and western Aleutian Arcs, both of which are located within the Russian Exclusive Economic Zone (E.E.Z.). Furthermore, what literature is available on these two areas is mainly in Russian and therefore difficult to access in the west. This is unfortunate because Kamchatka is one of the most volcanically active regions on Earth (Churikova et al., 2001) and there is strong evidence that parts of the Kurile Arc are equally active suggesting that this arc has the potential to host vigorous submarine hydrothermal systems. However, evidence for this activity is based largely on the study of G.M. Gavrilenko (1997) which deals exclusively with the occurrence of submarine ferromanganese crusts on various island arcs in the Pacific, of which crusts from the central and southern Kurile Arc make up only a part. Furthermore, this study was limited in scope and does not cover all the aspects which might reasonably be expected in a modern study of such deposits. Submarine hydrothermal activity has also been investigated in Kraternaya Bight, a submerged caldera located on Ushishir island in the central part of Kurile Arc. Although much effort was expended in this area by V.G. Tarasov et al. (1990), focussing mainly on biological aspects, this work has resulted in only one major publication in English. Submarine hydrothermal activity and mineralization have also been reported from Piip volcano in the western Aleutian Arc based, in part, on the results of dives of the Mir submersible (Bogdanov and Sagalevich, 2002). In this case, the results were published exclusively in Russian. The results of the studies of these three hydrothermal systems can therefore be classified as provisional and not readily accessible in the west. However, when the geological setting of the Kurile Arc is taken into account, it is clear that at least part of this region has the potential to be a frontier area for the study of world-class submarine hydrothermal systems. We therefore present the available data, much of it in translation and appearing in English for the first time, as a baseline for future studies there.

2. Geological setting of the Kurile arc

The Kurile island chain stretches from Kamchatka in the north to Hokkaido in the south, a distance of about 600 km (Sergeyev and Krasny, 1987). 44 subaerial volcanoes and hydrothermal fields have been reported to occur on 19 islands together with a further 5 submarine volcanoes (Anon, 2002, 2005). These submarine volcanoes are all poorly documented and it is probable that others remain undiscovered. In fact, this is a conservative estimate. Avdeiko et al. (1991) and Avdeiko (1993) have charted 105 subaerial and 100 submarine volcanoes along the arc (Fig. 1). In addition, 5 submarine caldera located west of Onekotan, Urup and Iturup were reported by Bondarenko (1991, 1992) and Bondarenko and Rashidov (2003). Major references on the volcanoes of the Kuril islands include Bezrukov et al. (1958), Gorshkov (1958, 1970), Erlich (1986), Avdeiko and Rashidov (1992) and Avdeiko et al. (1992). Sergeyev and Krasny (1987) have also prepared a comprehensive geological and geophysical atlas of the Kurile–Kamchatka region.

In the western Pacific, the Pacific Plate is subducted beneath the Okhotsk Plate (Kamchatka to central Honshu) and the Philippine Plate (Izu-Bonin and Mariana Arcs) and the Philippine Plate beneath the Eurasian Plate (Ryukyu Arc) (Wei and Seno, 1998). The rate of subduction of the Pacific Plate beneath the Okhotsk Plate along the Kurile Arc is 90 mm yr^{-1} in the north and 100 mm yr^{-1} in the south (Inoue and others 1987). The Pacific Plate is subducted normal to the Kurile Trench in the northern sector of the arc but obliquely in the southern sector of the arc south of Boussole Strait which lies between the islands of Simushir and Chirpoi (Kimura, 1986; DeMets, 1995). This induces a westward migration of the Kurile forearc sliver located in the Kurile forearc (Kimura, 1986; Taira, 2001). As a result, the volcanic islands in the northern sector of the arc form a linear chain whereas those in the southern sector of the arc are arranged en echelon (Kimura, 1986). The fast subduction in the southern part of the arc has resulted in the generation of earthquakes with magnitudes of about 8 along the southern Kurile trench during the last two centuries (Nanayama et al., 2003). Kasahara et al. (1997) have shown that the main aftershock distributions of these earthquakes in the southern Kuriles region are bounded by the Nossapu and Iturup Fracture Zones which lie perpendicular to the Kurile Trench and intersect Kunashir and Iturup at about their mid-points and act as barriers to seismicity. Like the Izu-Bonin, Mariana and Ryukyu Arcs, the Kurile Arc has no accretionary prism (von Huene and Scholl, 1991).

Overall, the Kurile Arc is seismically and volcanically much more active than the Izu-Bonin–Mariana and Ryukyu Arcs to the south with the most intense seismicity recorded in the southern sector of the arc at a longitude of 147–148°E which lies on the northward extension of a line marking the offset of marine magnetic anomaly patterns on the seafloor of the Pacific Plate (Nishikawa et al., 1987; Inoue et al., 1987; Tarakanov, 1987; Haghipour, 2001). Significantly, Haňus and Vaněk (1984c, Fig. 12a) have shown an offset of the palaeotrench corresponding to

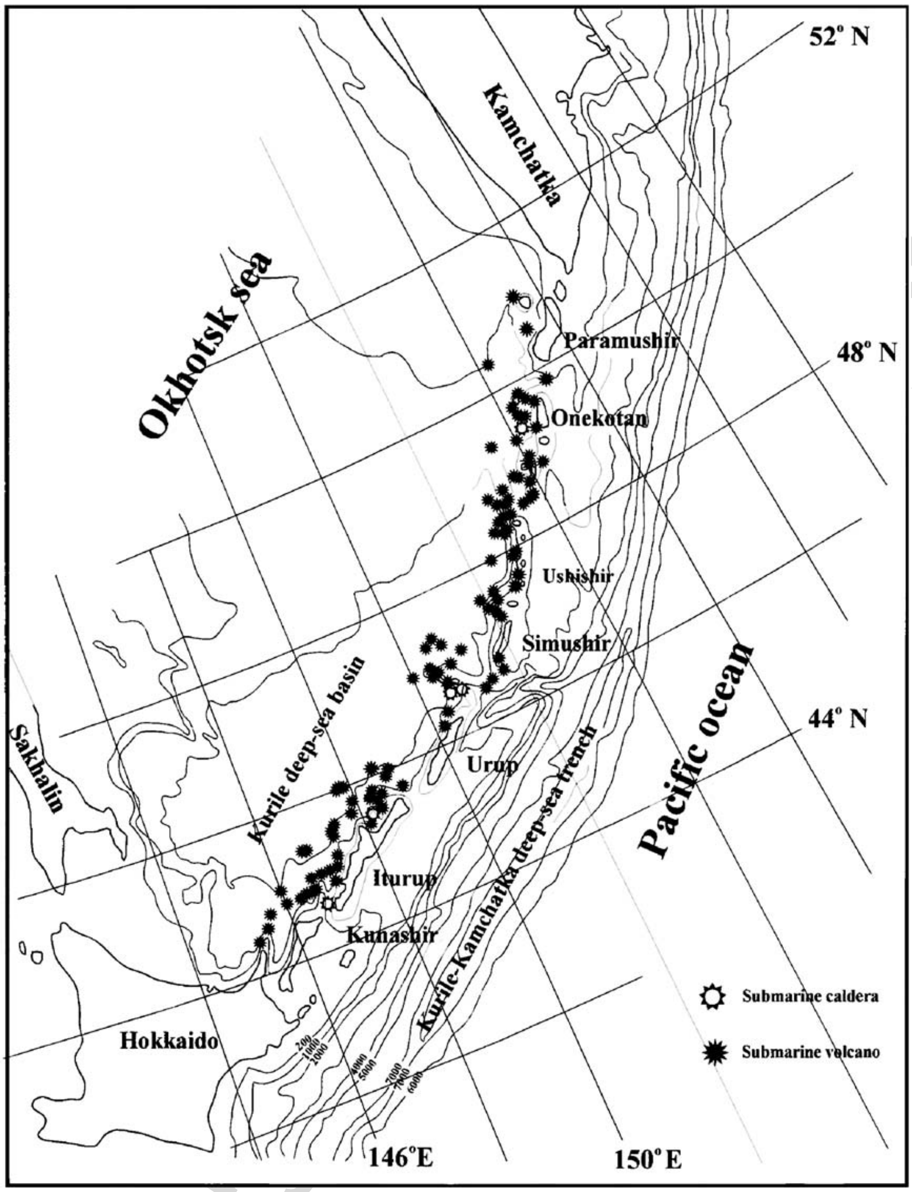

Fig. 1. Shows the locations of 100 submarine volcanoes (closed circles) and 5 submarine caldera (open circles) along the Kurile Arc. 81% of these volcanoes are in the rear arc (after Avdeiko et al., 1992).

longitudes of 146° 30′E to 151° 30′E at the active volcanic arc which may possibly be related to this zone of higher seismicity. The Kurile Arc is also marked by a sharp bend in the region of Boussole Strait (Avdeiko et al., 1991). By contrast, the northern Kuriles are structurally more similar to southern Kamchatka than to the rest of the arc (Kostenko et al., 1998). The Aleutian Arc is also seismically active in the central and eastern sectors of the arc but much less so in the western sector of the arc in the vicinity of the Vulcanologists Massif where Piip volcano is located (Moore, 1990, 1992).

The role of subduction in the evolution of the Kurile Arc has been documented by a number of authors (Haňus and Vaněk, 1984a,b,c, 1985, 1988; Bailey et al., 1987; Avdeiko et al., 1991; Ryan et al., 1995; Bailey, 1996). In particular, Haňus and Vaněk (1984a,b,c, 1985, 1988) established that the dip of the subducting Pacific slab varies from 31° beneath Kamchatka to 37° in the central Kuriles and 36° in the southern Kuriles and Hokkaido and that the Wadati–Benioff zone in this region is typically 50–65 km deep. Avdeiko et al. (1991) have shown that the Kurile Arc is actually made up of two parallel arcs, a frontal arc with a seismo-focal zone at a depth of 110–140 km and a rear volcanic arc with a seismo-focal zone at a depth of 160–190 km. It was established that more than 55% of all volcanoes are located on the frontal arc and only 20–25% on the rear arc. However, only 13% of the volcanoes in the frontal arc are submarine compared to 81% in the rear arc (Avdeiko et al., 1991; Ishikawa and Tera, 1997). The locations of these submarine volcanoes (including submarine caldera) are shown in Fig. 1.

Quaternary and Neogenic volcanic rocks from the Kurile Arc are typical andesite formations (Fedorchenko et al., 1989). The petrology of submarine volcanic rocks has been studied by Ostapenko and Kichina (1977) and Ostapenko (1979). Petrological variations have been observed across the arc (Bailey et al., 1987, 1989; Zhuravlev et al., 1987; Avdeiko et al., 1991; Ryan et al., 1995; Bailey, 1996). These have been attributed to the dehydration of amphibole, 14Å-clinochlore and serpentine at the fore arc and of phlogopite and 7Å-clinochlore at the rear arc (Avdeiko et al., 1991). The dominant rock types within the arc are medium K calc-alkaline lavas with As and Sb contents decreasing across arc (Ryan et al., 1995; Ishikawa and Tera, 1997). There is strong evidence that at least some of the volcanism is controlled by the presence of faults or fractures within the crust (Haňus and Vaněk, 1985, 1988; Avdeiko et al., 1991).

The nature of magmatic gases has been studied at Kudryavy volcano, a 996 m high basaltic–andesitic volcano (Tolstykh et al., 1997), located in Medvezhy (Bear) crater on the island of Iturup which is located in the southern sector of the arc (Taran et al., 1995). Fumarolic discharges are vapour rich with temperatures of up to 940 °C. Such high temperatures reflect the presence of a near-surface magma which has been estimated to lie about 80 m below the surface of the volcano (Botcharnikov et al., 2003). It was suggested that the magma may have risen close to the surface about 100 years ago during the last eruption and has remained there since. This has resulted in a large output of volatiles including at least 10^6 t yr^{-1} of water as well as a large number of minor elements such as Cd, Pb, W and As (Taran et al., 1995) and Pb, Mo, Bi, Sn, In, As, Se and Te (Wahrenberger et al., 2002). Pure rhenium sulfides with a formula $Re_{1.5-2.0}S$ (Korzhinsky et al., 1994) as well as native metals such as Al, Si, Ti, Fe and Pt (Korzhinskii et al., 1996) have been sampled in the sublimates from this volcano (Petrachenko, 1995). According to Fisher et al. (1998), the Kudryavy vent also emits 18,300 t yr^{-1} of CO_2 to the atmosphere of which 67% is derived from subducted marine carbonate, 21% from subducted organic matter and 12% from the mantle. These authors also calculated that 0.07 km^3 of mantle and subducted material would have been required to maintain the observed flux of volatiles over the 100 year period of high-temperature fumarolic activity. On Kamchatka, the Mutnovsky geothermal area is considered to be one of the most active thermal areas in the world with active volcanoes and high-temperature geothermal areas covering an area of 30 km^2 (Taran et al., 1992).

3. Submarine hydrothermal deposits from the Kurile arc

Since their discovery at Esmeralda submarine volcano on the Mariana Arc in 1978 (Gavrilenko, 1981; Gorshkov et al., 1982) and on the Tonga–Kermadec island arc in 1981 (Cronan et al., 1982; Moorby et al., 1984), submarine hydrothermal manganese deposits in island arcs have been reported in the Aeolian Arc (Eckhardt et al., 1997), the Izu-Bonin Arc (Usui and Someya, 1997; Usui and Glasby, 1998; Usui and Iizasa, 2002) and the Mariana Arc (Hein et al., 1997). In this paper, we will describe the distribution, morphology and composition of submarine hydrothermal iron and manganese deposits from the vicinity of Iturup on the Kurile island arc and from Piip submarine volcano in the western Aleutian arc. The report on the submarine hydrothermal minerals in the Kurile arc is taken mainly from Gavrilenko and Khramov (1989) and Gavrilenko (1997).

Submarine hydrothermal deposits were recovered mainly off the west coast to Iturup, the largest island in the Kurile chain. Iturup itself is characterized by the presence of 9 volcanoes or volcanic complexes (Demon, Chirip, Baransky, Bogatyr Ridge, Astonupuri, Lvinaya Past and Berutarube (all stratovolcanoes), Medvezhy (a somma volcano), the Golets–Tornyi Group of pyroclastic cones and the Grozny Group of complex volcanoes plus one unnamed submarine volcano 45° 2′N, 147° 12′E (see earlier) (Anon, 2002). In addition, a number of geothermal fields are located on Iturup such as the Okeanskoye geothermal field on the Pacific coast near Baransky volcano where a 6 MW geothermal power station has been built (Kononov, 2002).

Previous work on submarine hydrothermal ferromanganese crusts in the Kurile arc is restricted to that of Orlov (1982) who studied handpicked samples from only four stations. The ferromanganese deposits studied here were sampled during cruises 15 and 17 of *R/V Volcanolog* in 1982 and 1983. Sampling was carried out near the summits of submarine volcanoes and on volcanic ridges by dredge. Fig. 2 shows the locations of the samples described in this study.

At the Vavilov (Stn B15-87), Archangelsky (Stn B15-91) and Obruchev (Stns B17-9, 10 and 11) submarine volcanoes, at an unnamed submarine volcano 5 km NNE of Vavilov (Stns B17-8) and on the submarine ridge which is located south from Simushir island (Stn B17-44, 45 and 46), the rock samples consisted mainly of angular debris of andesite but included basalt, andesite–basalt, andesite–

dacite and dacite. From the submarine volcanoes situated on the western slopes of Urup and Iturup islands (Stns B17-15, 16, 17, 20, 23, 25, 38, 40, 41, and 43), the material consisted of angular debris varying in composition from basalt to dacite. The rocks were mainly fresh pillow-lavas, some of which had been hydrothermally altered with encrustations of sulfur along fissures.

Ferromanganese deposits were represented by two principal morphological types: nodules at Stns B15-87, B17-41, 44 and 46 and crusts at Stns B15-87 and 91 and B17-9, 10, 15, 16, 17, 20, 23, 38, 43, 44 and 46. In addition, sand and gravel cemented by Fe and Mn oxyhydroxides were sampled at Stn B17-20 and pumice and organic remains impregnated by Fe and Mn oxyhydroxides were sampled almost everywhere.

In addition to the results presented here, Anikeeva et al. (in press) have recently reported on a detailed mineralogical and chemical study of ferromanganese crusts taken from a number of seamounts located west of Paramushir Island and from a volcanic ridge located west of Edelstein Island in the northern sector of the Kurile Arc which were sampled during a cruise of *R/V Volcanolog* in 1991.

4. Chemical and mineralogical analysis

Selected samples of the collected material were analyzed by means of chemical and mineralogical methods including atomic absorption analysis, optical microscopy (investigation of the internal structure of the ferromanganese crusts and optical constants of minerals in polished thin-sections), X-ray diffraction (DRON-1, CoKα at 24 kV, 3 mA) and scanning electron microscopy (JEM-100C with KEVEX-5100) at the Institute of Oceanology, Russian Academy of Sciences, Moscow. In addition, wet chemical analysis and spectral analysis were carried out at the Institute of Volcanology, Petropavlovsk and X-ray

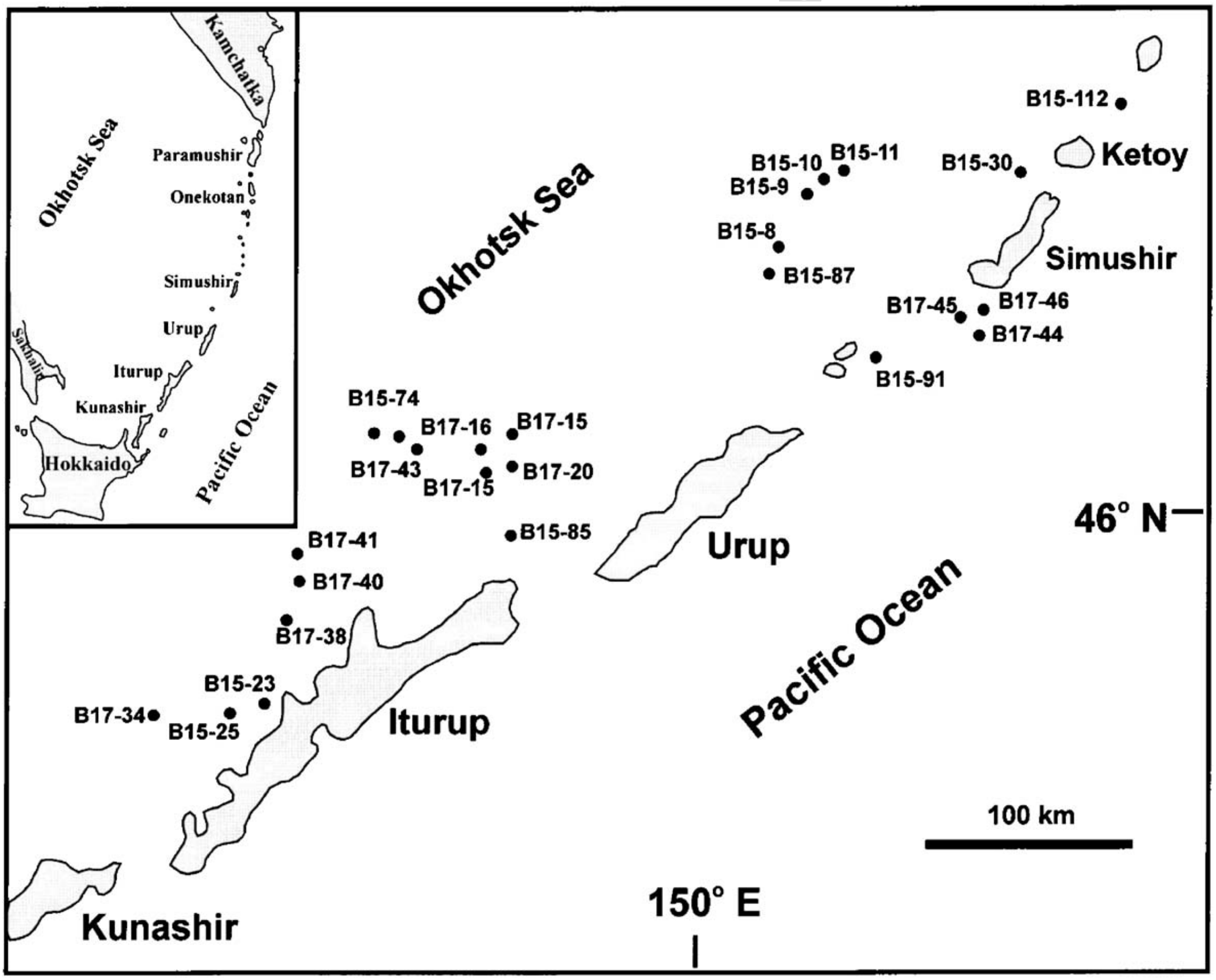

Fig. 2. Shows the positions of sampling stations on submarine volcanoes and ridges in the southern half of the Kurile Arc where submarine hydrothermal iron and manganese deposits were recovered. Only the positions of those stations where samples are mentioned in the text or listed in the tables are shown. The samples were taken mainly to the west of Simushir, Urup and Iturup islands. The inset shows the locations of the islands on the Kurile Arc (after Gavrilenko, 1997).

diffraction at the Institute of Mineral Resources, Novosibirsk. For X-ray diffraction analysis, both powdered samples at room temperature and samples heated to 100 °C were analyzed for the identification of buserite and todorokite.

5. Morphology

From the macroscopic character, internal structure and mineralogy of the samples, it was possible to distinguish three types of ferromanganese deposits in the Kurile Arc.

First type (Stns B17-44 and 46) consisted of black crusts and nodules composed of Mn oxides displaying smooth to botryoidal surface texture and a complex internal structure. Usually, the *basal layer* of the crusts consisted of debris (0.5–2 mm in diameter) cemented with a highly-reflecting manganese-rich material composed mainly of birnessite with lesser amounts of vernadite and rare occurrences of asbolane–buserite and goethite. Based on electron microprobe analysis, birnessite and vernadite were shown to contain Mg, K and Ca and asbolane–buserite Al and sometimes Si. The low concentration of Ni in these minerals differentiates them from deep-sea manganese nodules which are characterized by the high concentrations of Ni as well as the rare occurrence of asbolane–buserite which is one of the main components in deep-sea nodules.

Above the basal layer is a 30 mm thick crust consisting of radial mammillae with diameters of 0.5–2 mm cemented by thin layers of Mn oxides composed mainly of birnessite. On breaking, the basal layer material is seen to be steel-grey with a metallic luster. In some places, these massive layers have a structure typical of that of todorokite aggregates such as observed in manganese crusts from the Japan Sea (Skornyakova et al., 1987). The mammillae are dull black in appearance. They are composed of finely dispersed aggregates of birnessite and vernadite with minor amounts of lamellar particles of todorokite partly altered to vernadite. The replacement of todorokite by vernadite can be easily observed by SEM and XRD since the appearance of the todorokite particles is markedly different from that of vernadite but it is more difficult to establish whether the transformation of birnessite into vernadite had taken place because of the very similar appearance and diffraction patterns of these minerals.

The *upper layer* consisted of thin dendrites partly cemented with dense massive material. In appearance and mineral composition, it is identical to the cement of the basal layer. XRD analysis showed that the dendrites consist mainly of 14 Å birnessite and todorokite which is characterized by the absence of Mg in some particles whereas K and Na are always present. Such a mineral association is not characteristic of deep-sea manganese nodules and crusts but has previously been found in hydrothermal manganese crusts from the Atlantis Fracture Zone in the Atlantic Ocean (Chukrov et al., 1979) and the Tadjura Rift in the Gulf of Aden (Gorshkov et al., 1987). In the sample from Stn B17-46, the upper part of the crust consisted of an 8 mm thick dense layer formed by the interstratification of thin black and thicker steel-grey layers.

Second type consisted of crusts made up mainly of green and yellowish-green clay, brown veinlets and Mn oxides formed on a sediment substrate (Stns B15-87, B17-9, -10, -11, -17 and -25).

Green or yellowish-green clay formed a dense mass of cementing debris or semi-lithified stratified deposits. XRD analysis showed the clay minerals to be nontronite ($Na_{0.3}Fe^{3+}_2(Si,Al)_4O_{10}(OH)_2 \cdot nH_2O$). Based on electron microprobe analysis, the main components of this mineral were shown to be Fe, Si and K with minor amounts of Ca, Mg and Al and the clay often had a brownish colour. In these samples, feroxyhyte (δ-FeOOH) was also found. The gradual changes in colour (from yellowish-green to brown) in the surface zone and near the fissure area and the absence of Mn in feroxyhyte which is typical for hydrogenetic precipitation of this mineral showed that the feroxyhyte formed by oxidation of precursor minerals.

Brown veinlets interpenetrated the nontronite (Stns B17-9, 10 and 11) and were filled with an amorphous Fe–Si phase containing minor amounts of ferroxyhyte. In electron diffraction patterns, the ferroxyhyte displays diffuse reflections. The most recent mineralization consists of layers of birnessite (1.5 mm thick) crossing Fe–Si veinlets and dendrites of birnessite containing minor amounts of todorokite. Mn oxides also formed thin films on debris and foraminiferal shells.

Thin fissures in the dense nontronite crusts were infilled with black massive Mn oxides. Al could also be found in the clay groundmass. The massive Mn oxides were represented by todorokite and plate-like particles of 7 Å birnessite with minor amounts of 14 Å birnessite and vernadite. All these phases had similar contents of K, Ca and Mg. In some particles of todorokite, Mg was absent.

At Obruchev Seamount (Stns B17-9, -10, -11), the crusts were up to 50 mm thick and displayed variegated colouration due to the irregular alternation of black, brown, ocherous and green layers. These crusts apparently formed close to submarine hydrothermal vents with the formation of different layers reflecting changing physico-chemical conditions in the hydrothermal fluids.

Third type of nodules and crusts were composed of Mn and Fe oxyhydroxides displaying different structure, mineralogy and chemical composition from the first type of deposit (Stns B15-91, B17-15, 16, 20, 23, 38, 40, 41 and 43). At Stn B17-43, crusts up to 50 mm thick with a mammilated surface texture were recovered.

The *base* of the thickest crusts consisted of particles cemented with black massive Mn oxides which were composed mainly of birnessite and todorokite with minor amounts of 14 Å birnessite and vernadite. Some particles of todorokite were partly altered to vernadite. Todorokite was often seen to intergrow 14 Å birnessite.

The *upper part* of these crusts was characterized by interlayering of thin layers of brown ore and light-coloured clays. The ore substance in the crust consisted of thin layers of collomorphous material and thicker layers. Such a structure is typical of hydrogenous deep-sea manganese crusts and nodules. Electron diffraction studies showed that these layers consisted of vernadite, feroxyhyte and goethtite. The thin-bedded part of the crust was similar to deep-sea nodules in terms of composition (Mn/Fe < 2.5). P and Ba are characteristically enriched in vernadite and feroxyhyte in the upper part of these crusts. In some crusts (Stn B17-17), the layers are composed of asbolane–buserite, buserite-1, birnessite and random todorokite and buserite-II in lesser amounts in those parts of the crust which had contact with sediment. Ni was present in all these minerals.

6. Chemical composition

The chemical composition of selected samples of ferromanganese deposits from individual sampling stations is shown in Table 1. The samples show wide variability in composition with Mn varying from 0.06 to 39%, Fe from 0.32 to 27%, Co from 20 to 1230 ppm, Ni from < 50 to 4000 ppm, Cu from < 20 to 300 ppm and Zn 270 to 1100 ppm. For comparison, the average composition of the ferromanganese deposits in the Kurile Arc is compared with the average concentration of Pacific Ocean deep-sea nodules (Andreev, 1994) and with the average concentration of Co-rich Mn crusts from the equatorial NW Pacific (Hein, 2004).

In principle, Co-rich Mn crusts should give a better indication of the composition of hydrogenous manganese deposits than deep-sea nodules because they are formed on a substrate and are not therefore in direct contact with the underlying sediment. However, in the

Table 1
Chemical composition of submarine ferromanganese deposits from the Kurile arc. Mn and Fe in %; Co, Ni, Cu and Zn in ppm (Gavrilenko, 1997)

Stn N.	Lat (°E)	Long (°N)	Water depth (m)	Mn	Fe	Co	Ni	Cu	Zn	Mn/Fe
B17-8	46° 59.9′	150° 30.1′	1200–1250	15.6	7.4	190	520	90	440	2.1
B17-9	47° 06.7′	150° 28.5′	960–1200	1.9	26.1	50	<50	30	270	0.07
B17-11a	47° 06.9′	150° 28.4′	1140–1240	10.6	14.0	80	320	40	710	0.75
B17-11b	47° 06.9′	150° 28.4′	1140–1240	0.06	24.3	40	<50	<20	310	0.002
B17-11c	47° 06.9′	150° 28.4′	1140–1240	0.7	27.0	60	<50	50	590	0.03
B17-15	45° 56.2′	148° 39.9′	900–1100	11.1	12.5	660	2530	190	780	0.89
B17-16	45° 56.4′	148° 39.8′	830–1200	15.2	13.7	1130	2600	170	890	1.1
B17-17	46° 00.1′	148° 45.0′	1040–1300	9.6	11.6	120	520	50	390	0.83
B17-20	45° 53.6′	148° 47.2′	1110–1200	1.5	6.2	120	400	90	350	0.24
B17-23	45° 02.5′	147° 12.8′	770–780	12.3	17.1	960	2700	200	830	0.72
B17-25	45° 01.7′	147° 01.5′	350–600	11.5	20.9	1230	2700	180	880	0.55
B17-38	45° 17.2′	147° 25.6′	330–550	4.2	22.8	160	320	30	600	0.19
B17-40	45° 27.7′	147° 27.7′	1150–1200	29.6	2.3	110	190	50	290	12.8
B17-41	45° 32.1′	147° 29.3′	670–800	13.7	18.3	700	900	80	800	0.75
B17-43	46° 01.0′	147° 56.2′	1500–1650	10.4	15.0	570	1920	300	850	0.69
B17-44	46° 32.5′	151° 50.8′	880–990	25.8	3.3	750	540	90	550	7.8
B17-45	46° 33.7′	151° 47.5′	900–950	5.2	11.8	490	120	160	840	0.44
B17-46a	46° 33.0′	151° 50.3′	680–860	18.7	7.7	310	1220	160	920	2.4
B17-46b	46° 33.0′	151° 50.3′	680–860	39.0	0.3	70	570	80	1100	122
B15-87	46° 52.8′	150° 29.0′	680–760	6.7	6.5	20	190	130	860	1.0
B15-91	46° 25.6′	151° 13.2′	590–640	4.3	9.6	310	430	70	590	0.45
B15-112	47° 30.6′	152° 49.1′	40	4.1	21.2	<30	<50	50	460	0.004
Av.	–	–	–	11.3	13.6	370	860	110	650	0.83
Pacific Ocean nodules (Andreev, 1994)	–	–	–	19.6	12.2	2800	6500	4700	1400	1.6
Co-rich Mn crusts (Hein, 2004)				22.4	16.7	5665	4266	1023	692	1.3

The average compositions of the Pacific Ocean manganese nodules (Andreev (1994) and of Co-rich Mn crusts from the equatorial NW Pacific (Hein, 2004) are listed for comparison.

vicinity of the oxygen minimum zone (OMZ), Co is enriched in the Co-rich crusts relative to deep-sea nodules because the deposition rate of Mn at the OMZ is at a minimum whilst the deposition rate of Co remains constant. Cu, on the other hand, is depleted in the crusts because $CuCl_3^-$ becomes the stable form of Cu in seawater under the less oxidizing conditions at the OMZ resulting in a lower deposition rate of Cu from seawater (Glasby, 2006). Of the elements considered, only Mn, Fe, Ni and Zn in the Co-rich crusts can therefore be considered to be hydrogenetic in origin in the strict sense of the term.

On average, the Mn/Fe ratio of the Co-rich Mn crusts is much higher than that of the ferromanganese deposits in the Kurile Arc reflecting the presence of nontronite in the Kurile Arc deposits as well as the fractionation of Mn from Fe in the submarine hyrothermal manganese deposits (Table 1). Zn is also uniformly high in the Kurile Arc deposits. The characteristic enrichment of Zn in the hydrothermal deposits is a consequence of Zn being the trace element most readily taken into solution during hydrothermal leaching (Toth, 1980).

On average, the concentration of Mn is also somewhat lower and the concentration of Fe somewhat higher in the Kurile arc ferromanganese deposits compared to those of the Pacific deep-sea nodules (Table 1). However, the concentrations of Co, Ni and Cu in the deep-sea nodules are several times higher than in the Kurile Arc deposits. This reflects the low concentrations of these elements in the hydrothermal iron and manganese deposits of the Kurile Arc and the absence of any significant diagenetic contribution to the crusts or nodules.

On the basis of the compositional data presented in Table 1, the ferromanganese deposits of the Kurile Arc can be divided into three end members; submarine hydrothermal manganese deposits characterized by Mn/Fe ratios >7 and low contents of Co, Ni, Cu and Zn, submarine hydrothermal iron deposits characterized by high Fe/Mn ratios > 10 and low contents of Co, Ni, Cu and Zn and samples characterized by intermediate Mn/Fe ratios and elevated contents of Co, Ni, Cu and Zn which can be considered to be dominantly hydrogenous in origin, although they may contain a significant hydrothermal component in some cases. Samples with Ni contents >1900 ppm may be considered to be hydrogenous in origin (Skornyakova, 1976). The compositional characteristics of these three types of ferromanganese deposit have been discussed by Glasby (2006).

On this basis of mineralogical and compositional, the *first type* of deposit can be considered to consist of typical submarine hydrothermal manganese crusts characterized by a massive structure and the absence of distinctive layering, high Mn/Fe ratios and low contents of Co, Ni and Cu with todorokite and birnessite present as the main Mn minerals.

The *second type* of deposit is characterized by high Fe/Mn ratios and low contents of Co, Ni and Cu (Gavrilenko and Khramov, 1989). It consists mainly of nontronite together with minor amounts of todorokite, birnessite and feroxyhyte. The association of nontronite with submarine hydrothermal iron and manganese deposits has previously been observed in submarine hydrothermal formations from the Galapagos Rise, Explorer Ridge and TAG hydrothermal fields (Moorby et al., 1984; Thompson et al., 1985; Lazur et al., 1986; Skornyakova et al., 1987).

The *third type* of deposit has a more complex mode of formation. The *base* of the crusts consists of black massive Mn oxides composed mainly of birnessite and todorokite which are typical of submarine *hydrothermal deposits* of the *first type*. The upper thin-bedded parts of the crusts, on the other hand, are characterized by intermediate Mn/Fe ratios, high contents of Co, Ni and Cu and the occurrence of Mn–feroxyhyte, Fe–vernadite, asbolane–buserite, buserite-I and buserite-II. These features are typical of *hydrogenous deposits* and reflect the declining influence of the hydrothermal contribution to the crusts, possibly as a result of migration of the site of deposition away from the active volcanic arc as

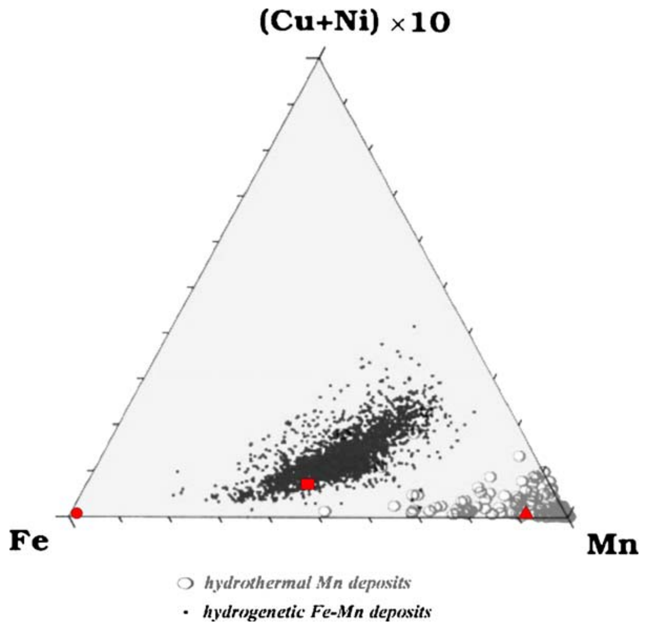

Fig. 3. Shows a triangular plot of (Cu+Ni)–Mn–Fe for hydrogenous Fe–Mn deposits and hydrothermal Mn deposits from the N.W. Pacific (after Usui and Someya, 1997). Superimposed on this diagram are plots of the extreme hydrothermal Mn deposit (B17-40) (solid triangle), the extreme hydrothermal Fe (nontronite) deposit (B17-11b) (solid circle) and the extreme hydrogenous Mn deposit (B17-16) (solid square) from the Kurile Arc.

observed, for example, on the Izu-Bonin Arc (Usui and Someya, 1997; Usui and Glasby, 1998; Usui and Iizasa, 2002).

In order to confirm the validity of the above assignments, the compositions of the extreme end members of each of these three types of deposit were plotted on the triangular diagram of Usui and Someya (1997). This shows that the hydrothermal Mn, hydrothermal Fe and hydrogenous Mn deposits lie within the fields designated by these authors (Fig. 3). Because the hydrogenous Mn deposits mainly overlie preexisting hydrothermal Mn deposits, it follows that there would have been a negligible diagenetic contribution to their formation. This is confirmed by the Ni + Cu contents of these samples which are typical of hydrogenous Mn deposits.

The principal characteristics of each type of deposit are briefly summarized in Table 2.

7. Submarine hydrothermal activity in Kraternaya Bight, Kurile Arc

Ushishir volcano is situated at the central part of Kuril island chain and is represented by two small islands: Riponkicha in the north and Yankicha in the south. These two islands are the remains of the large shield volcano 10 km in diameter (Gorshkov, 1971). Yankicha island has a circular rim with a diameter of more than 1.5 km in which a submerged caldera (Kraternaya Bight) with a diameter of ~ 1 km and maximum depth of 63 m has formed. A narrow strait connects this caldera with the open ocean. Ushishir volcano experienced historic eruptions in 1710, 1769 and 1884 (Anon, 2002, 2005). The 1769 eruption was a submarine eruption from a vent near the centre of the caldera and formed a lava dome. Nowadays the Ushishir volcano is in the stage of solfatar activity (Marhinin and Stratula, 1977; Gavrilenko et al., 1989). The hydrothermal activity is associated with fault zones as demonstrated by geophysical investigations.

Shallow-water hydrothermal fields and areas of seeping hydrothermal fluids have been reported in Kraternaya Bight (Tarasov et al., 1990; Gavrilenko, 1997; Gamo and Glasby, 2003). Subaerial volcanic activity characterized by boiling springs (92–96 °C) occurs in the intertidal zone in the southeastern part of the bight. These volcanic waters are acidic (pH 2–3.5) and contain high concentrations of H_2S (up to 340 μM), other reduced sulfur compounds, ammonia, silica (up to 3 mM), phosphorus, and 2–3 orders of magnitude higher concentrations of Mn, Fe, Zn, Cu, Cd, Ni, and Cr than seawater. Mixing with seawater and ground water has resulted in low-temperature hydrothermal fluids with temperatures in the range 10–43 °C and pH of 6–7. Around the perimeter of the bay are numerous gas vents and areas where hydrothermal fluid with a temperature of 10 to 34 °C is seeping through the seafloor at depths of 0 to 22 m. The major components of the vent gases are CO_2 (54–66%) and N_2 (27–42%). The effects of the hydrothermal fluid inflow are reflected as distinctive peaks of CO_2, pH, and H_2S in the water column.

Bacterial, algobacterial and diatom mats occur on sloping areas of the crater floor where hydrothermal fluids were seeping as well as near gasohydrothermal vents (Tarasov et al., 1990). These mats were thought to

Table 2
Summary descriptions of the three types of ferromanganese deposits recovered from the Kurile Arc

Description	Type 1	Type 2	Type 3
	Hydrothermal manganese crusts	Nontronite	Hydrothermal manganese crusts overlain by hydrogenous manganese oxides
Morphology	Upper layer consists of cemented massive material Intermediate layer consists of thin Mn oxides Basal layer consists of steel grey material with dense metallic lustre	Dense layer consists of green or yellowish clay occurring as lithified stratified deposits Thin fissures in the crust infilled with black massive Mn oxides	Upper part of crust consists of allomorphous material similar to that found in hydrogenous manganese oxides Base of crusts consists of black massive Mn oxides
Mineralogy	Upper layer consists of 14 Å birnessite and todorokite Intermedite layer consists of birnessite and vernadite Basal layer consists of birnessite and vernadite	Nontronite ($Na_{0.3}Fe_2^{3+}(Si,Al)_4O_{10}(OH)_2\cdot nH_2O$).plus feroxyhyte (δ-FeOOH)	Upper part of crusts consists of vernadite, feroxyhyte and goethtite Base of crusts consists mainly of birnessite and todorokite
Composition	High Mn/Fe ratios and low contents of Co, Ni and Cu	High Fe/Mn ratios and low contents of Co, Ni and Cu	Upper part of crusts displays intermediate Mn/Fe ratios, and high contents of Co, Ni and Cu Base of crusts displays high Mn/Fe ratios and low contents of Co, Ni and Cu

serve as biogeochemical filters which transform the hydrothermal trace elements and reduced compounds into sedimentary organic matter. In particular, the 5 mm thick algobacterial mats have a multi-layered structure which includes many microorganisms (different kinds of sulfur oxidizing bacteria and thermophylic archaebacteria) and are characterized by extremely high rates of CO_2 fixation and organic matter production (up to 33.4 gC m^{-2} d^{-1}). The influence of both chemosynthetic and photosynthetic pathways may result in complicated metabolic and energy cycles. The bottom macrofauna have a high population density and biomass (up to 10 kg m^{-2}).

Sediment thickness within the crater was estimated to be in the range 80–120 m based on a study of seismic records (Gavrilenko, 1997). The upper layer of the sediments ranged from 1 mm to 0.27 m thick and consisted mainly of fine sandy silt in which oxidizing conditions prevail. The lower layer consisted of sandy and fine sandy silt which smelt of H_2S indicating reducing conditions. An interesting feature is the occurrence of Fe–P crusts in the sediments (Gavrilenko and Khramov, 1989). These crusts are generally a few centimetres in diameter, 1–3 mm thick, fine layered with layers of different colours ranging from almost black to brown ochre and are enriched in Fe and P with P concentrations of up to 5%. The associated sediments are also enriched in Fe (3.8–11%) and P (0.05–1.8%) but contain low contents of Mn (0.05–0.18%). The elevated Fe and P concentrations in the crusts and sediments relative to volcanic rocks from Ushishir (Gavrilenko, 1997) and sediments from the Sea of Okhotsk (Ilyev et al., 1979)

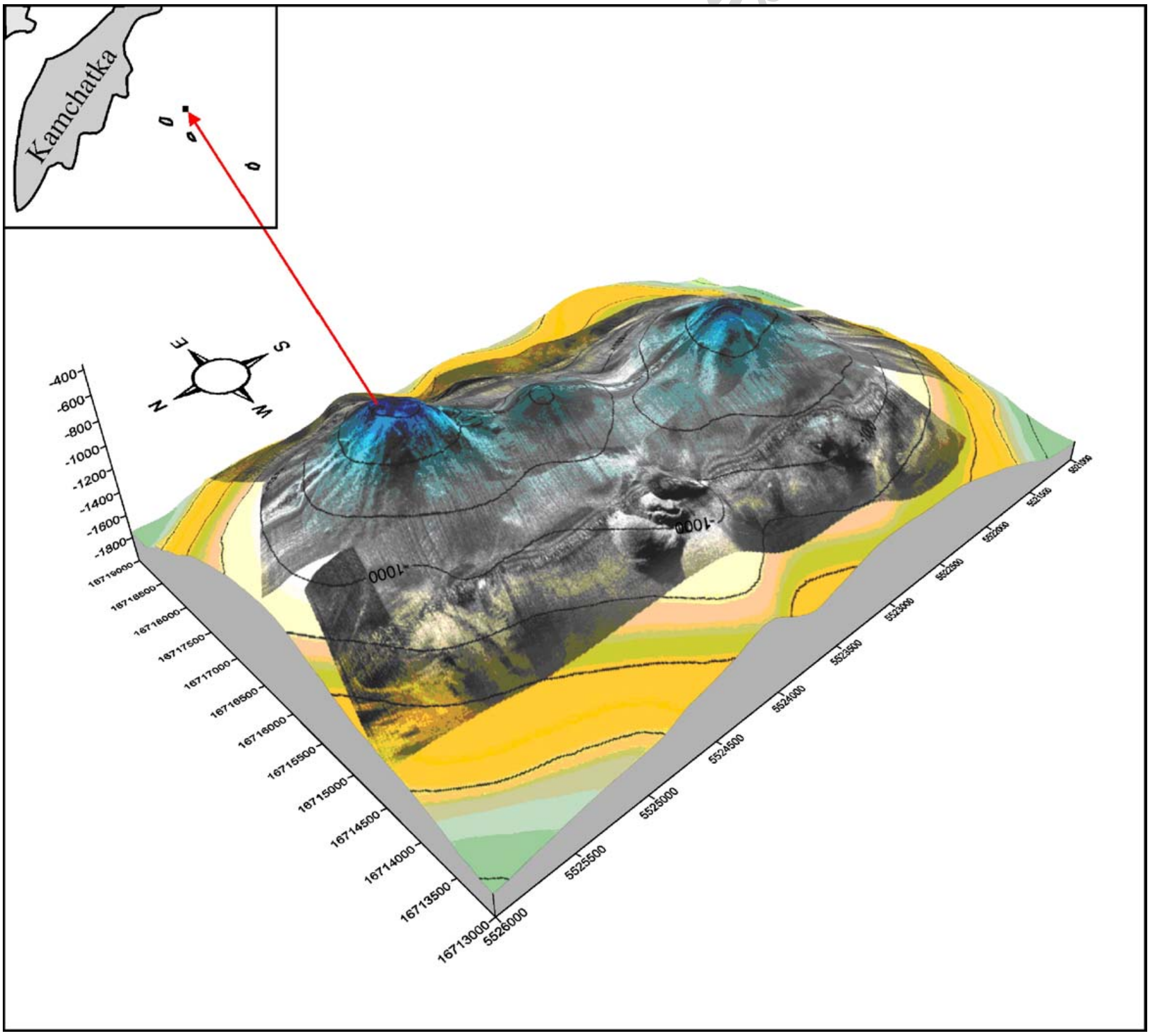

Fig. 4. Is a mosaic of side-scan profiles showing the three principal peaks on Piip volcano.

suggest that the Fe and P are mainly hydrothermal in origin, although the uptake of P from seawater on freshly-precipitated Fe oxyhydroxides cannot be discounted. However, the low concentration of Mn precludes a hydrothermal origin for this element. This situation is similar to that encountered in the Santorini caldera on the Aegean Arc where the hydrothermal Fe oxyhydroxides have deposited mainly within the caldera whereas much of the dissolved Mn has been swept out to sea (Boström et al., 1990; Papavassiliou et al., 1990; Cronan et al., 2000).

8. Submarine hydrothermal deposits from Piip submarine volcano, western Aleutian Arc

Piip volcano is an active submarine volcano characterized by a dacite–rhyolite association located at 55° 25′ N, 167° 20′E in the southern part of the Komandorskaya depression of the western Aleutian Arc about 40 km north of Bering island (Tsvetkov, 1991; Anon, 2005). It is located in an area of relatively low seismicity compared to the central Aleutian and southern Kurile Arcs (Inoue et al., 1987; Tarakanov, 1987). The volcano was discovered during the 21st cruise of *R/V Volcanolog* in 1984 and subsequently explored during the 26th (1986), 28th (1987), 32nd (1988), 35th (1989) and 39th (1991) cruises of *R/V Volcanolog* and the 22nd cruise (1990) of *R/V Academician M. Keldysh* in conjunction with the submersible Mir (Seliverstov, 1988; Seliverstov et al., 1986, 1991, 1995; Bogdanova et al., 1990; Gavrilenko, 1997; Bogdanov and Sagalevich, 2002).

Piip volcano is located on the central part of Volcanologists Massif which rises 4000 m above the deep-sea floor. The massif intruded into a major NNE–SSW-oriented graben. Both the graben and massif are relatively young and were formed as a result of back-arc spreading. The volcano has three summits: northern, central and southern (Fig. 4). The northern and southern summits are considerably larger than the central summit and have summit craters. The northern crater has a diameter 300 m and the southern crater 500 m. The volcanoes consist of andesite–dacite, dacite and pumice.

The first sign of submarine hydrothermal fluid discharge in the form of a gas plume above the volcano was recorded on the echo-sounder in 1987. Subsequent submersible studies showed that hydrothermal activity at the northern crater took the form of shimmering water and jet-like vent fluids emanating from a water depth of about 382 m. Hydrothermal discharge was estimated to have had a velocity of 0.05–0.1 m s^{-1}, a flow diameter of 0.1 m and an output of 50–100 l min^{-1}. Although the maximum measured temperature was 133 °C (the upper limit of the

Table 3
Chemical compositions of intermediate-temperature deposits from Piip volcano

	Anhydrite, gypsum	Anhydrite, gypsum	Anhydrite, gypsum	Gypsum, anhydrite	Opal, pyrite, kaolinite	Calcite, quartz, gypsum	Aragonite, calcite, gypsum	Pyrite, calcite, gypsum	Barite	Barite, calcite
SiO_2	n.d.	tr.	n.d.	tr.	35.8	0.70	n.d.	0.16	1.3	0.13
TiO_2	n.d.	0.02	0.06	n.d.	0.30	n.d.	0.02	n.d.	n.d.	n.d.
Al_2O_3	0.23	0.17	1.01	0.10	10.2	0.40	0.06	0.14	0.74	0.42
Fe_2O_3	0.22	0.55	0.27	0.20	5.5	1.2	0.18	n.a.	0.40	0.24
FeS	n.a.	n.a.	n.a.	n.a.	42.3	n.a.	n.a.	84.8	n.a.	n.a.
MnO	n.d.	n.d.	n.d.	n.d.	n.d.	0.20	n.d.	0.02	0.03	n.d.
MgO	0.58	0.44	0.30	0.42	n.d.	0.44	0.44	0.15	0.88	0.29
CaO	40.9	39.5	39.1	33.9	n.d.	53.8	52.2	4.3	0.30	1.60
Na_2O	0.68	0.68	0.74	0.36	0.52	0.58	0.72	0.22	0.58	0.28
K_2O	n.d.	n.d.	0.03	n.d.	0.35	n.d.	0.03	0.04	0.03	0.03
H_2O^-	1.8	0.90	0.80	n.d.	0.60	n.d.	n.d.	0.90	0.50	0.50
H_2O^+	n.d.	n.d.	n.d.	15.5	3.40	n.a.	4.5	n.a.	n.d.	n.d.
P_2O_5	n.d.	n.d.	n.d.	n.d.	0.05	0.26	n.d.	1.8	n.d.	n.d.
BaO	n.d.	n.d.	n.d.	n.d.	n.d.	n.d.	n.d.	n.d.	61.1	60.6
CO_2	n.d.	0.30	n.d.	n.d.	n.d.	40.4	40.8	2.7	8.5	1.26
SO_3	54.6	56.3	56.8	49.8	na	1.9	0.48	n.a.	23.4	31.6
F	0.23	n.d.	0.15	n.d.	0.30	n.d.	0.15	0.23	0.19	0.35
Cl	0.22	0.22	0.06	n.d.	0.28	0.22	0.06	0.06	0.22	0.22
Sr	0.25	0.13	0.21	0.12	0.04	0.01	0.23	0.01	1.7	0.70
Sum	99.7	99.2	99.7*	100.4	100.7**	100.2	99.9	100.2***	99.9	98.2

All elements in % (Sagalevich et al., 1992). FeS_2 was determined by wet chemical analysis of S and Fe(II).
Notes: 1. Main minerals are underlined.
2. n.d. not detected, n.a. not analyzed, tr. trace.
Sum includes *0.13% PbO, **1.16% Cu, ***3.0% As + 1.2% Sb + 0.57% Hg.

Table 4
Chemical composition of four types of low-temperature hydrothermal iron and manganese deposits sampled from the southern crater of Piip submarine volcano at 55° 22.6′ N; 167° 15.2′ E depth 590–760 m and 55° 23.9′ N, 167° 14.4′ E depth 890–975 m

	Nontronite	Fe oxyhydroxides	Hisingerite	Manganese crusts
Mn	0.06	0.70	1.8	39.9
Fe	14.0	20.0	3.4	1.2
Al	4.4	3.3	6.4	1.4
Ti	0.14	0.11	0.23	0.05
Cr	50	18	26	8
Li	11	12	22	12
Mo	40	40	60	30
V	5	45	68	28
Sr	250	690	500	30
Cd	5	7	7	5
Pb	6	12	16	4
Co	270	240	400	20
Ni	36	59	220	280
Cu	12	13	30	16
Zn	47	94	130	220
Mn/Fe	0.004	0.035	0.54	32

Mn, Fe, Al and Ti in %; all other elements in ppm (Bogdanova et al., 1990; Gavrilenko, 1997).

temperature measurement system), there were indications that the actual fluid temperature may have reached 250 °C (Seliverstov et al., 1995). Most of the gas discharged from the vents consisted of thermogenic methane (>80%) (Sagalevich et al., 1992). Many bacterial mats were discovered, mostly coloured white and more rarely dark gray, brown and orange, as well as hydrothermal macrofauna (giant clams, *Calyptogena*).

Submarine hydrothermal minerals displaying a variety of forms were recovered. Based on their temperature of formation, the hydrothermal minerals could be divided on two types, intermediate-temperature sulfate, carbonate, amorphous silica and pyrite sampled from the northern crater by submersible and low-temperature iron and manganese deposits sampled from the slopes and summit of the volcano.

Six types of *intermediate-temperature deposits* could be distinguished:

1. Anhydrite chimneys from the northern summit which have a height of 1.5 m and a width of 0.4 m.
2. Semi-lithified crusts consisting of gypsum which overlie the dacites close to the vents of the northern summit.
3. Barite coated with black ferromanganese oxyhydroxides was sampled at distances of several meters from the vent on the southern summit.
4. Non-lithified deposits in the vicinity of the vents of northern summit which consisted of amorphous

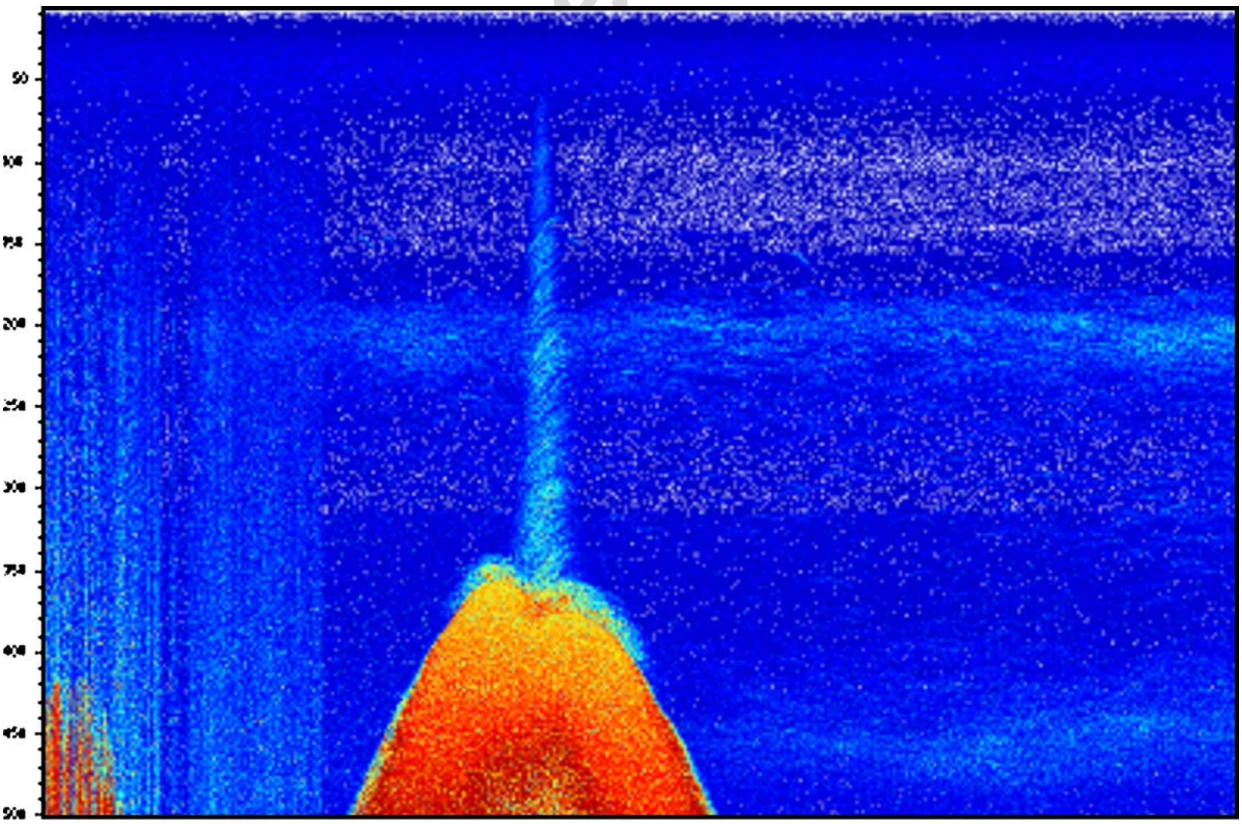

Fig. 5. Is an echo-sounder profile showing a gas plume rising from a water depth of about 382 m above the northern crater of Piip volcano.

silica, pyrite (up to 40%) with minor amounts of kaolinite.
5. A large mound-like hydrothermal edifice (up to 10 m in height) on the southern summit which consisted of calcite and barite with small chimneys on top composed mainly of calcite and aragonite.
6. Small crystals of pyrite (0.5 mm) coating the inner surfaces of the cavities in these chimneys.

The chemical compositions of these types of intermediate-temperature deposits are presented in Table 3. It should be noted that the pyrite encrustations are extremely enriched in As (3.0%), Sb (1.2%) and Hg (0.57%). Electron microprobe analyses of pyrites from different host minerals also showed enrichment for As, Sb and Hg as well as extraordinarily high concentrations of silver (up to 6%) in pyrite from barite mineralization (Torokhov, 1992).

During cruise 26 of *R/V Volcanolog*, samples of hydrothermal ferromanganese deposits were also recovered from the periphery of the hydrothermal fields on the slopes and summit of the volcano. These deposits generally overlay pumice or infilled fissures and cavities within it. Nontronite also infilled the cavities and impregnated the groundmass of the pumice. Fe oxyhydroxides on the surface of the pumice were always overlain by black Mn deposits. All the pumice samples were hydrothermally altered, intensively fissured and easily broken. The porosity of the pumice was up to 50 vol.% and the pore size varied from several up to 20–30 mm.

Four types of *low-temperature iron and manganese deposits* were distinguished visually and mineralogically

1. yellowish-green mineral aggregates and grayish green crusts infilling cavities within pumice and partly interpenetrating the groundmass such that the whole sample becomes grayish-green. Nontronite was the dominant mineral type in these samples;
2. orange-yellow and rusty infillings up to 2 mm thick within the fissures. These consisted of poorly crystalline Fe oxyhydroxides in which ferrihydrite was sometimes determined, possibly formed by the crystallization of Fe oxyhydroxides,
3. thin brown coatings on the surface of the pumice consisting of hisingerite ($Fe_2^{3+}Si_2O_5(OH)_4 \cdot 2H_2O$) with minor amounts of quartz. The hisingerite occurred as fibrous aggregates and was possibly formed as the result of alteration of iron silicates following the oxidation of Fe^{2+} to Fe^{3+}. Quartz was deposited as a late-stage precipitate,
4. 1–3 mm thick black manganese crusts covering the surfaces of the rocks in which birnessite was the principal mineral phase.

The chemical compositions of the four types of *low-temperature hydrothermal* deposit are presented in Table 4. The nontronite and Fe oxyhydroxides were formed by direct precipitation from hydrothermal fluids (Severmann et al., 2004), possibly assisted by bacterial activity in the case of nontronite (Koski et al., 2003).

In 2004, a cruise of *R/V Professor Khromov* was undertaken to Piip submarine volcano as part of a joint Russian–American Expedition 'Rusalka'. During this cruise, side-scan profiling was carried out to map the morphology of the volcanic massif, special echo-sounding profiling of the water column was undertaken to detect the presence of gas plumes above the summit of volcano and rocks and submarine hydrothermal minerals were sampled. Fig. 4 shows a 3-D image of Piip volcano obtained by side-scan profiling and Fig. 5 confirms that vigorous submarine hydrothermal activity is presently taking place in the northern crater. Samples of andesitic rocks, pumice and tuff impregnated and coated by Fe–Mn–hydroxides <1 mm thick and small fragments of low-temperature barite were recovered from the volcano by dredging.

9. Discussion

Submarine hydrothermal manganese crusts are generally considered to have precipitated last in the sequence sulfide mineral associated with silicates and oxides, sharply fractionated oxides and silicates of localized extent and widely dispersed ferromanganese oxides and may therefore be considered to be late-stage, low temperature hydrothermal deposits (Rogers et al., 2001; Kuhn et al., 2003a,b). The submarine hydrothermal manganese deposits recovered from the Kurile Arc during the course of this study were formed at relatively shallow water depths (<1650 m). Perhaps the best comparison of the submarine hydrothermal deposits of the Kurile Arc can be made with submarine hydrothermal manganese and sulfide deposits from the seismically less active Izu-Bonin Arc to the south (Usui and Glasby, 1998; Iizasa et al., 1999, 2004; Glasby et al., 2000; Usui and Iizasa, 2002). In this case, recent hydrothermal manganese crusts associated with active hydrothermal systems tend to occur on seamounts or in rifts located about 5–40 km behind the volcanic front. Fossil hydrothermal manganese crusts are generally overlain by hydrogenous manganese crusts. The thickness of the overlying hydrogenous crusts depends on the length of time since hydrothermal activity ceased.

In their earlier study, Gavrilenko and Khramov (1989) concluded that submarine hydrothermal iron and manganese deposits were recovered only in the southern half of the Kurile Arc based on dredging operations carried out along the length of the arc. This finding was in agreement with the conclusion of Avdeiko and Krasnov (1988) that the extensive development of submarine hydrothermal activity occurs mainly in the southern part of the arc. However, the recent results of Anikeeva et al. (in press) demonstrate that all three types of submarine hydrothermal and hydrogenous manganese and iron deposits reported in this study are found in the northern sector of the arc. These deposits therefore appear to occur along the length of the arc.

Five submarine caldera are located along the Kurile Arc west of Onekotan, Urup and Iturup. Submarine hydrothermal sulfides are often found in submarine caldera. A good example of this type of mineralization is the Sunrise deposit which is located in the caldera of Myojin Knoll on the Izu-Bonin Arc at a water depth of 1210–1360 m. This deposit contains approximately 9×10^6 t of massive sulfides with an average composition of 21.9% Zn, 2.3% Pb, 1210 ppm Ag and 20 ppm Au putting in the top 20% of the world's kuroko deposits by size (Iizasa et al., 1999). However, the five caldera located on Kurile Arc all occur at relatively shallow water depths. The one off Onekotan occurs at a water depth of 700 m, the two off Urup at 300 m, the one at the northern end of Iturup at 300 m and the one at the southern end of Iturup at 580 m. As a consequence, subsurface boiling would have occurred during the ascent of the hydrothermal fluid resulting in the deposition of sulfide minerals beneath the seafloor in all five caldera (Ishibashi and Urabe, 1995). These caldera would therefore most probably be characterized by the occurrence of sulfate rather than sulfide chimneys. However, the southern Kurile Arc is amongst the seismically most active submarine volcanic arcs in the world (Addicott and Richards, 1982). As such, it might reasonably be expected that the two caldera located west of Iturup Island would be characterized by intense submarine hydrothermal activity such as found in the SPOT area (Southernmost Part of the Okinawa Trough) in the southern Okinawa Trough (Glasby and Notsu, 2003). Venting of the hydrothermal fluids may well be associated with ring faults located along the back wall of the crater as observed at Myojin Knoll (Iizasa et al., 1999). In addition, de Ronde et al. (2003b) have estimated that actively venting volcanoes occur with a frequency of one vent site for every 87 km of arc length along intraoceanic volcanic arcs based on a survey of 2900 km of these arcs. Since the Kuriles arc is about 600 km in length, this suggests that there should be about 7 active vent sites located along the Kuriles arc at present.

Kraternaya Bight is a shallow submerged caldera with a maximum depth of 63 m. Here, hydrothermal activity around the crater is largely fumarolic with maximum temperatures below boiling point. No hydrothermal vents were sampled but it is likely that these are of relatively low temperature precipitating mainly Fe oxyhydroxides on contact with seawater. Because the residence time of hydrothermal Mn in seawater is several years, about five orders of magnitude longer than that of hydrothermal Fe (Glasby, 2006), it follows that divalent Mn of hydrothermal origin would have been virtually all removed from the crater before Mn oxyhydroxides could form. In addition, boiling would almost certainly have taken place during the ascent of the hydrothermal fluids to the surface resulting in sulfide mineralization within the host rocks. Perhaps the principal interest in studying hydrothermal activity in Kraternaya Bight, however, lies in the influence of the hydrothermalism on the biota in the crater.

Piip submarine volcano in the western Aleutian Arc also appears to be very active with intermediate-temperature hydrothermal deposits located in the summit caldera of the seamount and low-temperature hydrothermal deposits from the periphery of the hydrothermal fields. The shallow depth of these craters implies that boiling of the ascending hydrothermal fluid has taken place precluding the deposition of sulfides at the summit of the volcano. Intermediate-temperature Ba–Ca–Si–Fe–Mn deposits such as found at Piip are rather common in the submarine hydrothermal fields of the southwest Pacific and have been reported in the North Fiji Basin (Bendel et al., 1993), Okinawa Trough (Halbach et al., 1993), Manus Basin (Bogdanov and Sagalevich, 2002), on Franklin Seamount in the Woodlark Basin (Hekinian et al., 1993; Bogdanov et al., 1997) and the Valu Fa Ridge in the Lau Basin (Herzig et al., 1990; Fouquet et al., 1993). In the North Fiji basin, Okinawa Trough and Lau Basin, they are associated with high-temperature massive sulfide deposits. The closest analogue to Piip volcano is Franklin Seamount where both low-temperature (ferromanganese) and intermediate-temperature (barite and amorphous silica with minor amounts of sulfides) deposits have been reported in the summit caldera. Bogdanov et al. (1997) have suggested that subsurface deposition of massive sulfides below the low- and intermediate-temperature mineralization zones may have occurred. The high concentrations of As (>1000 ppm) in the Fe–Mn–Si mineralization of Franklin Seamount may also be an evidence that these massive subsurface sulfide deposits contain high concentrations of Au and Ag (Boyd et al., 1993).

As shown in Table 2, the concentrations of As and Hg in pyrite-bearing mineralization from Piip volcano reach 3% and 0.57%, respectively, in some cases. These high concentrations of As and Hg in the pyrite suggest the influence of phase separation on the hydrothermal system since both elements are known to fractionate into the vapour phase during boiling. A similar situation has been observed at the Grimsey hydrothermal field north of Iceland (Hannington et al., 2001; Kuhn et al., 2003b). In general, barite-bearing hydrothermal mineralization is characterized by high gold and silver concentrations (Hannington et al., 1991).

10. Conclusions

The Kurile Arc consists of at least 100 submarine volcanoes and 5 submarine caldera located mainly in the rear arc. The arc is seismically very active, particularly in the south, and is characterized by extensive volcanism and hydrothermal activity. Three types of submarine hydrothermal mineralization were recovered from the submarine volcanic summits from the southern and central parts of Kurile Arc in the vicinity of Iturup, Urup and Simushir islands. These consist of hydrothermal manganese crusts, nontronite and hydrothermal manganese crusts overlain by hydrogenous manganese oxides. From the preceding discussion, it is clear that Kurile Arc has the potential to host submarine hydrothermal systems and associated submarine hydrothermal mineralization analogous to that discovered at other volcanic arcs in the western Pacific such as the Izu-Bonin and Tonga–Kermadec Arcs. In the caldera located west of Iturup, it is anticipated that intense hydrothermal activity such as found in the SPOT area in the southern Okinawa Trough will occur.

Hydrothermal activity was also discovered at the Piip submarine volcano located in the western Aleutian Arc. It is characterized by intermediate- and low-temperature hydrothermal minerals with associated bacterial mats and giant clams. The maximum measured temperature of the hydrothermal fluids was 133 °C, although the actual temperature may have reached 250 °C. Based on the shallow water depth of the Piip hydrothermal field, the formation of subsurface sulfide deposits would be expected.

At present, information on submarine hydrothermal activity and mineralization in the Kurile and Aleutian Arcs is extremely limited. Future studies should therefore focus on identifying submarine hydrothermal systems in these two regions and evaluating the controls on their formation. Based on experience gained during many Russian cruises, the following methods of exploration are recommended for prospecting for hydrothermal areas, near-bottom horizontal profiling of the water column by CTD with nephelometer and methane sensor, geoelectrical profiling, shallow drilling and heat flow measurements.

Acknowledgements

We are grateful to the crew members of *R/V Vulcanolog* and Professor Khromov cruises, to Dr. Kathy Crane, chief scientist of the of 'Rusalka' expedition, and the geological team of this expedition headed by Dr. Anatoly Astakhov for collecting the samples and data on which this study is based. This study was supported by RFBR grants (05-05-65102, 06-05-96002, 06-05-96129) and FEB RAS grant (06-III-A-08-326).

References

Addicott, H.W., Richards, P.W., 1982. Plate-tectonic map of the Circum-Pacific region Pacific Basin sheet. Circum-Pacific Council for Energy and Mineral Resources (Map).

Andreev, S.I., 1994. Metallogeny of Ferromanganese Formations of the World Ocean. Nedra, St.-Petersburg. 189 pp (In Russian with extended summary in English).

Anikeeva, L.I., Gavrilenko, G.M., Rashidov, V.A., Semkova, T.A., Cherkashov, G.A., in press. Ferromanganese crusts of underwater massive Edelstein and underwater volcano close to Paramushir Island. Volcanol. Seisomol. No. 6, (in Russian).

Anon, 2002. Volcano World (http://www.volcanoworld.org).

Anon, 2005. Global Volcanism Program Volcanic Activity Reports, Smithsonian National Museum of Natural History (http://www.volcano.si.edu).

Avdeiko, G.P., 1993. Submarine vulcanism of Kurile Arc. Dr Sci. thesis, Moscow. 66 pp. (in Russian).

Avdeiko, G.P., Krasnov, S.G., 1988. Sulfide ores and their association with submarine volcanoes and thermal springs in island arcs. Volcanol. Seismol. 7, 497–516.

Avdeiko, G.P., Rashidov, V.A., 1992. Geological setting of volcanoes of the Kurile Arc. In: Puscharovsky, Yu.M. (Ed.), Submarine Volcanism and Zonation of the Kurile Arc. Nauka, Moscow, pp. 7–28 (in Russian).

Avdeiko, G.P., Volynets, O.N., Antonov, A.Yu., Tsvetkov, A.A., 1991. Kurile island-arc volcanism: structural and petrological aspects. Tectonophysics 199, 271–287.

Avdeiko, G.P., Volynets, O.N., Rashidov, V.A., 1992. Catalogue of submarine volcanoes of the Kurile Arc. In: Puscharovsky, Yu.M. (Ed.), Submarine Volcanism and Zonation of the Kurile Arc. Nauka, Moscow, pp. 29–227 (in Russian).

Bailey, J.C., 1996. Role of subducted sediment in the genesis of Kurile–Kamchatka island arc basalts; Sr isotopic and elemental evidence. Geochem. J. 30, 289–321.

Bailey, J.C., Larsen, O., Frolova, T.I., 1987. Strontium isotope variations in Lower Quaternary volcanic rocks from the Kurile island arc. Contrib. Mineral. Petrol. 95, 155–165.

Bailey, J.C., Frolova, T.I., Burikov, I.A., 1989. Mineralogy, geochemistry and petrogenesis of Kurile island-arc basalts. Contrib. Mineral. Petrol. 102, 265–280.

Baker, E.T., Feely, R.A., de Ronde, C.E.J., Massoth, G.J., Wright, I.C., 2004. Submarine hydrothermal venting on the southern Kermadec volcanic arc front (offshore New Zealand): location and extent of particle plume signatures. In: Larter, R.D., Leat, P.T. (Eds.), Intra-oceanic subduction systems: tectonic and magmatic processes. Geol. Soc. Spec. Publ., vol. 219, pp. 141–161.

Bendel, V., Fouquet, Y., Auzende, J.-M., Lagabrielle, Y., Grimaud, D., Urabe, T., 1993. The White Lady hydrothermal field, North Fiji back-arc basin, Southwest Pacific. Econ. Geol. 88, 2237–2250.

Bezrukov, P.L., Zenkevich, N.L., Kanaev, V.F., Udintsev, G.B., 1958. Submarine seamounts and volcanoes of Kurile Arc. Proc. Lab. Vulcanol. 13, 71–88.

Bogdanov, Yu.A., Sagalevich, A.M., 2002. Geologic investigations with deep submersibles MIR. Scientific World, Moscow. 304 pp. (in Russian).

Bogdanov, Yu.A., Lisitzin, A.P., Binns, R.A., Gorshkov, A.I., Gurvich, E.G., Drits, V.A., Dubinina, G.A., Bogdanova, O.Yu., Sivkov, A.V., Kuptsov, V.M., 1997. Low-temperature hydrothermal deposits of Franklin seamount, Woodlark Basin, Papua New Guinea. Mar. Geol. 42, 99–117.

Bogdanova, O.Yu., Gorshkov, A.I., Baranov, B.V., Seliverstov, N.I., Sivstov, A.V., 1990. Hydrothermal deposits from Piip submarine volcano, Komandorskii Basin. Volcanol. Seismol. 11, 354–373.

Bondarenko, V.I., 1991. New submarine caldera nearby Onekotan island, The Kurile islands. Volcanol. Seismol. 12, 418–421.

Bondarenko, V.I., 1992. Seismoacoustic investigations in L'vinaya Past' caldera. Volcanol. Seismol. 13, 448–458.

Bondarenko, V.I., Rashidov, V.A., 2003. Cherny Bratya volcanic Mass (Kurile isles). Volcanol. Seismol. 3, 35–51 (in Russian).

Boström, K., Papavassiliou, C.T., Ingri, J., Kalogeropoulos, S., 1990. Geochemistry and structural control of hydrothermal sediments and new hot springs in the caldera of Santorini. In: Hardy, D.A. (Ed.), Thera and the Aegean World III, vol. 2. Thera Foundation, London, pp. 325–336.

Botcharnikov, R.E., Shmulovich, K.I., Tkachenko, S.I., Korzhinsky, M.A., Rybin, A.V., 2003. Hydrogen isotope geochemistry and heat balance of a fumarolic system: Kudriavy volcano, Kuriles. J. Volcanol. Geotherm. Res. 124, 45–66.

Boyd, T., Scott, S.D., Hekinian, R., 1993. Trace element patterns in Fe–Si–Mn oxyhydroxides at three hydrothermally active seafloor regions. Resour. Geol. Spec. Issue 17, 83–95.

Chukrov, F.V., Gorskhov, A.I., Sitsov, A.V., Berezovskaya, V.V., 1979. About new mineral phases in oceanic manganese micronodules. Proc. Acad. Sci. USSR, Geol. 1, 83–90 (in Russian).

Churikova, T., Dorendorf, F., Wörner, G., 2001. Sources and fluids in the mantle wedge below Kamchatka, evidence from across-arc geochemical variation. J. Petrol. 42, 1567–1593.

Cronan, D.S., Glasby, G.P., Moorby, S.A., Thomson, J., Knedler, K.E., McDougall, J.C., 1982. A submarine hydrothermal manganese deposit from the south-west Pacific island arc. Nature 298, 456–458.

Cronan, D.S., Varnavas, S.P., Hodkinson, R., 2000. Hydrothermal mineralizing processes and associated sedimentation in Santorini hydrothermal embayments. Mar. Georesour. Geotechnol. 18, 77–118.

DeMets, C., 1995. Oblique convergence and deformation along the Kuril and Japan trenches. J. Geophys. Res. 97, 17,615–17,617.

de Ronde, C.E.J., Baker, E.T., Masoth, G.J., Lupton, J.E., Wright, I.C., Feely, R.A., Greene, R.R., 2001. Intra-ocean subduction-related hydrothermal venting, Kermadec volcanic arc, New Zealand. Earth Planet. Sci. Lett. 193, 359–369.

de Ronde, C.E., Faure, K., Bray, C., Chappell, D.A., 2003a. Hydrothermal fluids associated with seafloor mineralization at the southern Kermadec arc volcanoes, offshore New Zealand. Mineral. Deposita 38, 217–233.

de Ronde, C.E.J., Massoth, G.J., Baker, E.T., Lupton, J.E., 2003b. Submarine hydrothermal venting related to volcanic arcs. In: Simmons, S.F., Graham, I.J. (Eds.), Volcanic, Geothermal, and Ore Forming Fluids: Rulers and Witnesses of Processes within the Earth. Soc. Econ. Geol. Spec. Publ., vol. 10, pp. 91–110.

Eckhardt, J.-D., Glasby, G.P., Puchelt, H., Berner, Z., 1997. Hydrothermal manganese crusts from Enareta and Palinuro Seamounts in the Tyrrhenian Sea. Mar. Georesour. Geotechnol. 15, 175–208.

Embley, R.W., Baker, E.T., Chadwick, W.W., Lupton, J.E., Resing, J.A., Massoth, G.J., Nakamura, K., 2004. Explorations of Mariana Arc volcanoes reveal new hydrothermal systems. EOS, Trans. Am. Geophys. Union 85 (4), 37–40.

Erlich, E.N., 1986. Geology of calderas of Kamchatka and Kurile Islands with comparison to calderas of Japan and Aleutians, Alaska. U.G. Geol. Surv. Open-File Rep. 86–291. 300 pp.

Fedorchenko, V.I., Abdurahmanov, A.I., Rodionova, R.I., 1989. Vulkanism of Kurile Arc: Geology and Petrogenesis. Nauka, Moscow. 237 pp. (in Russian).

Fisher, T.P., Giggenbach, W.F., Sano, Y., Williams, S.N., 1998. Fluxes and sources of volatiles discharged from Kudryavy, a subduction zone volcano, Kurile Islands. Earth Planet. Sci. Lett. 160, 81–96.

Fiske, R.S., Naka, J., Iizasa, K., Yuasa, M., Klaus, A., 2001. Submarine silicic caldera at the front of the Izu-Bonin Arc, Japan: voluminous seafloor eruptions of rhyolite pumice. GSA Bull. 113, 813–824.

Fouquet, Y., von Stackelberg, U., Charlou, J.L., Erzinger, J., Herzig, P.M., Mühe, R., Wiedecke, M., 1993. Metallogenesis in back-arc environments: the Lau Basin example. Econ. Geol. 88, 2154–2182.

Gamo, T., Glasby, G.P., 2003. Submarine hydrothermal activity in coastal zones. In: Taneguchi, M., Wang, K., Gamo, T. (Eds.), Land and Sea Hydrogeology. Elsevier, Amsterdam, pp. 151–163.

Gavrilenko, G.M., 1981. Esmeraldo submarine volcano and associated Fe–Mn ore formation. Volcanol. Seismol. 1, 51–55 (In Russian).

Gavrilenko, G.M., 1997. Under-water volcanic and hydrothermal activity as a source of metals in the ferromanganesian formations of the island arcs. Dal'nauka, Vladivostok. 165 pp. (In Russian).

Gavrilenko, G.M., Khramov, S.V., 1989. Ferromanganese formations of the submarine slopes of the Kuril Island Arc. Volcanol. Seismol. 8, 278–284.

Gavrilenko, G.M., Bondarenko, V.I., Sazonov, A.P., 1989. Marine volcanological explorations at Kraternaya Bay. Mar. Biol. 3, 19–28 (In Russian).

Glasby, G.P., 2006. Manganese: predominant role of nodules and crusts. In: Schulz, H.D., Zabel, M. (Eds.), Marine Geochemistry Second Edition. Springer-Verlag, Berlin, pp. 371–428.

Glasby, G.P., Notsu, K., 2003. Submarine hydrothermal mineralization in the Okinawa Trough, SW of Japan: an overview. Ore Geol. Rev. 23, 299–339.

Glasby, G.P., Iizasa, K., Yuasa, M., Usui, A., 2000. Submarine hydrothermal mineralization on the Izu-Bonin Arc, south of Japan: an overview. Mar. Georesour. Geotechnol. 18, 141–176.

Gorshkov, G.S., 1958. Kurile Islands catalog of active volcanoes of the World and Solfatara Fields, 7. IAVCEI, Rome, pp. 1–99.

Gorshkov, G.S., 1970. Volcanism and the upper mantle: investigations in the Kurile Island Arc. Plenum Press, N.Y. 385 pp.

Gorshkov, A.P., 1971. Volcanic activity of the Kuril Arc. Nauka, Moscow. 424 pp. (In Russian).

Gorshkov, A.P., Gavrilenko, G.M., Seliverstov, N.I., Scripko, K.A., 1982. Geologic structure and fumarolic activity of the Esmeralda submarine volcano. Internat. Symp. on the Activity of Oceanic Volcanoes. S. Miguel Azores, Ponta Delgada, pp. 271–298.

Gorshkov, A.P., Bogdanov, O.A., Sivtsov, A.V., 1987. Petrography and mineralogy of the ores from Tadjura Rift. Tadjura Rift Geology. Nauka, Moscow, pp. 65–78 (in Russian).

Haghipour, A. (General Co-ordinator) 2001. Seismotectonic Map of the World Scale 1: 25,000,000. Commission for the Geological Map of the World (Map).

Halbach, P., Pracejus, B., Marten, A., 1993. Geology and mineralogy of massive sulfide ores from the central Okinawa Trough, Japan. Econ. Geol. 88, 2210–2226.

Hannington, M.D., Herzig, P.M., Scott, S.D., 1991. Auriferous hydrothermal precipitates on the modern seafloor. In: Foster, R.P. (Ed.), Gold Metallogeny and Exploration. Blackie & Sons, Glasgow, pp. 249–282.

Hannington, M.D., Herzig, P.M., Stoffers, P., Scholten, J., Botz, R., Garbe-Schönberg, D., Jonasson, I.R., Roest, W., 2001. First observations of high-temperature submarine hydrothermal vents and massive anhydrite deposits off the north coast of Iceland. Mar. Geol. 177, 199–220.

Haňus, V., Vaněk, J., 1984a. Earthquake distribution and volcanism in Kamchatka, Kurile Islands, and Hokkaido Part 1: Kamchatka and northern Kuriles. Studia Geophys. Geod. 28, 36–55.

Haňus, V., Vaněk, J., 1984b. Earthquake distribution and volcanism in Kamchatka, Kurile Islands, and Hokkaido Part 2: central Kuriles. Studia Geophys. Geod. 28 (36–55), 129–148.

Haňus, V., Vaněk, J., 1984c. Earthquake distribution and volcanism in Kamchatka, Kurile Islands, and Hokkaido Part 3: southern Kuriles and Kamchatka. Studia Geophys. Geod. 28, 271.

Haňus, V., Vaněk, J., 1985. Structure of the Wadati–Benioff zones and volcanism produced by the process of subduction. Tectonophysics 112, 51–67.

Haňus, V., Vaněk, J., 1988. Deep structure, volcanism and the Wadati–Benioff zone of the northwestern Pacific convergent plate margin. J. Geodyn. 10, 25–41.

Hein, J.R., 2004. Cobalt-rich ferromanganese crusts: global distribution, composition, origin and research activities. Minerals other than polymetallic nodules of the international seabed area Proceedings of a workshop held on 26–30 June 2000 in Kingston, Jamaica, Volume 1, pp. 188–272.

Hein, J.R., Koschinsky, A., Halbach, P., Mamheim, F.T., Bau, M., Kang, J-K., Lubrich, N., 1997. Iron and manganese oxide mineralization in the Pacific. In: Nicholson, K., Hein, J.R., Bühn, B., Dasgupta, S. (Eds.), Manganese mineralization: Geochemistry and Mineralogy of Terrestrial and Marine Deposits. Geol. Soc. Spec. Publ., vol. 119, pp. 123–138.

Hekinian, R., Hoffert, M., Larqué, P., Chemineé, J.L., Stoffers, P., Bideau, D., 1993. Hydrothermal Fe and Si oxyhydroxide deposits from South Pacific intraplate volcanoes and East Pacific Rise axial and off-axial regions. Econ. Geol. 88, 2099–2122.

Herzig, P.M., von Stackelberg, U., Petersen, S., 1990. Hydrothermal mineralization for the Valu Fa Ridge, Lau back arc basin (SW Pacific). Mar. Min. 9, 271–301.

Iizasa, K., Fiske, R.S., Ishizuka, O., Yuasa, M., Hashimoto, J., Ishibashi, J., Naka, J., Horii, Y., Fujiwara, Y., Imai, A., Koyama, S., 1999. A kuroko-type polymetallic sulfide deposit in a submarine silicic caldera. Science 283, 975–977.

Iizasa, K., Sasaki, M., Matsumoto, K., Shiokawa, S., Tanahashi, M., on-board scientists, 2004. A first extensive huydrothermal field associated with kuroko-type deposit in a silicic caldera in a nascent rift zone, Izu–Ogasawara (Bonin), Japan. Oceans '04 MTS/IEEE Techno-Ocean '04 November 9–12, 2004 Kobe, Japan, pp. 991–996.

Ilyev, A.Ya., Voronova, V.A., Zaharova, M.A., et al., 1979. Seafloor sediments from the southern part of the Okhotsk Sea. Nauka, Moscow. 148 pp. (in Russian).

Inoue, E., et al., 1987. Plate-tectonic map of the Circum-Pacific region Northwest Quadrant. Circum-Pacific Council for Energy and Mineral Resources (Map).

Ishibashi, J.-i., Urabe, T., 1995. Hydrothermal activity related to arc magmatism in the western Pacific. In: Taylor, B. (Ed.), Backarc Basins: Tectonics and Magmatism. Plenum Press, N.Y, pp. 451–495.

Ishikawa, T., Tera, F., 1997. Source, composition and distribution of the fluid in the Kurile mantle wedge from across-arc variations of B/Nb and B isotopes. Earth Planet. Sci. Lett. 152, 123–138.

Kasahara, J., Sato, T., Mochizuki, T., Kobayashi, K., 1997. Paleotectonic structures and their influence on recent seismotectonics in the south Kuril subduction zone. Isl. Arc 6, 267–280.

Kimura, G., 1986. Oblique subduction and collision: forearc tectonics of the Kuril arc. Geology 14, 404–407.

Kononov, V.I., 2002. Geothermal resources of Russia and their utilization. Lithol. Miner. Resour. 2, 115–123.

Korzhinsky, M.A., Tkachenko, S.I., Shmulovich, K.I., Taran, Y.A., Steinberg, G.S., 1994. Discovery of a pure rhenium mineral at Kudriavy volcano. Nature 369, 51–52.

Korzhinskii, M.A., Tkachenko, S.I., Bulgakov, R.F., Shmulovich, K.I., 1996. Condensate compositions and native metals in sublimates in high-temperature gas streams of Kudryavyi Volcano, Iturup Island, Kurile islands. Geochem. Int. 34, 1057–1064.

Koski, R., German, C.R., Hein, J.R., 2003. Fate of hydrothermal products from mid-ocean Ridge hydrothermal systems. In: Halbach, P.E., Tunnicliffe, V., Hein, J.R. (Eds.), Energy and Mass Transfer in Marine Hydrothermal Systems. Dahlem University Press, Berlin, pp. 316–335.

Kostenko, N.P., Korchuganova, N.I., Dunaeva, N.N., 1998. Modern geological structure of Kuriles–Kamchatka region. Oceanology 38, 293–394.

Kuhn, T., Bostock, B.C., Koschinsky, A., Halbach, P., Fendorf, S., 2003a. Enrichment of Mo in hydrothermal Mn precipitates: possible Mo sources, formation process and phase associations. Chem. Geol. 199, 329–343.

Kuhn, T., Herzig, P.M., Mau, S., Hannington, M.D., Jonasson, I.R., 2003b. The Grimsey field: a shallow-marine hydrothermal system north of Iceland. In: Eliopoulos, et al. (Ed.), Mineral Exploration and Sustainable Development. Millpress, Rotterdam, pp. 139–142.

Lazur, Yu.M., Varentsov, I.M., Ermilov, V.V., 1986. Dispersed Mn–Fe–Ti–Cu–Zn mineralization in hydrothermal and pelagic deposits from Galapagos Rift zone (70th cruise of "Glomar Challenger"). Geochem. Int. 23 (6), 151–157.

Marhinin, Eu.K., Stratula, D.S., 1977. Hydrothermal activity in the Kuril Islands. Nauka, Moscow. 212 pp. (In Russian).

Massoth, G.J., de Ronde, C.E.J., Lupton, J.E., Feely, R.A., Baker, E.T., Lebon, G.T., Maenner, S.M., 2004. Chemically rich and diverse submarine hydrothermal plumes of the southern Kermadec volcanic arc (New Zealand). In: Larter, R.D., Leat, P.T. (Eds.), Intra-oceanic subduction systems: tectonic and magmatic processes. Geol. Soc. Spec. Publ., 219, pp. 119–139.

Moorby, S.A., Cronan, D.S., Glasby, G.P., 1984. Geochemistry of hydrothermal Mn-oxide deposits from the S.W. Pacific island arc. Geochim. Cosmochim. Acta 48, 433–441.

Moore, G.W., 1990. Geodynamic map of the Circum-Pacific Region Arctic Sheet. Circum-Pacific Council for Energy and Mineral Resources (Map).

Moore, G.W., 1992. Plate-tectonic map of the Circum-Pacific Region Arctic Sheet. Circum-Pacific Council for Energy and Mineral Resources (Map).

Nanayama, F., Satake, K., Furukawa, R., Shimokawa, K., Atwater, B., Shigeno, K., Yamaki, S., 2003. Unusually large earthquakes inferred from tsunami deposits along the Kurile Trench. Nature 424, 660–663.
Nishikawa, C., et al.,1987. Geodynamic map of the Circum-Pacific region Northwest Quadrant. Circum-Pacific Council for Energy and Mineral Resources (Map).
Orlov, A.A., 1982. Fe–Mn forms from Okhotsk sea. Geological settings of Okhotsk sea region. Far East Sciences Center of the Academy of Sciences of USSR, Vladivostok, pp. 101–106 (in Russian).
Ostapenko, V.F., 1979. Submarine volcanoes of Kurile Arc and geological evolution of Kuriles–Kamchatka region. Rep. Russ. Acad. Sci. 242, 168–171.
Ostapenko, V.F., Kichina, E.N., 1977. Petrology of Kurile Islands. Geolology of Far East Seas. Vladivostok, pp. 24–45.
Papavassiliou, C., Boström, K., Paritsis, S., Galanopoulos, V., Arvantides, N., Kalogeropoulos, S., 1990. Drilling in an ore-forming shallow hydrothermal system, Santorini Volcano, Greece. In: Hardy, D.A. (Ed.), Thera and the Aegean World III, vol. 2. Thera Foundation, London, pp. 250–256.
Petrachenko, E.D., 1995. Mineralization of the Kuril Island arc. Resour. Geol. Spec. Issue 18, 271–276.
Rogers, T.D.S., Hodkinson, R.A., Cronan, D.S., 2001. Hydrothermal manganese deposits from the Tonga–Kermadec Ridge and Lau Basin region, Southwest Pacific. Mar. Georesour. Geotechnol. 19, 245–268.
Ryan, J.G., Morris, J.D., Tera, F., Leeman, W.P., Tsvetkov, A., 1995. Cross-arc geochemical variations in the Kurile arc as a function of slab depth. Science 270, 625–627.
Sagalevich, A.M., Torokhov, P.V., Matveenkov, V.V., Galkin, S.V., Moskalev, L.I., 1992. Hydrothermal deposits of the Piip volcano (Bering Sea). Proceedings of Academy of Sciences of the USSR. Geology, vol. 9, pp. 104–114 (in Russian).
Seliverstov, N.I., 1988. Seabed structure near Kamchatka and geodynamic joint zone Kurile–Kamchatka and Aleutian Arcs. Nauka Mir, Moscow. 164 pp. (in Russian).
Seliverstov, N.I., Avdeiko, G.P., Ivanenko, A.N., et al., 1986. New submarine volcano in the west part of Aleutian Arc. Volcanol. Seismol 4, 3–16 (in Russian).
Seliverstov, N.I., Gavrilenko, G.M., Kiryanov, V.Yu., 1991. Modern activity of Piip volcano, Komandorsky Basin. Volcanol. Seismol. 11, 757–779.
Seliverstov, N.I., Torohov, P.V., Baranov, B.V., 1995. Piip submarine volcano: the structure-tectonic control, geological settings and hydrothermal activity. Volcanol. Seismol. 2, 50–71 (in Russian).
Sergeyev, K.S., Krasny, M.L. (Eds.), 1987. Geology–Geophysical Atlas of the Kuril–Kamchatka Island System. Ministry of Geology of the USSR, Academy of Sciences of the USSR Ministry of Gas industry of the USSR, Leningrad. 36 sheets (in Russian and English).
Skornyakova, N.S., 1976. Chemical composition of Fe–Mn nodules from the Pacific Ocean. Nauka, Moscow, pp. 190–204 (in Russian).
Skornyakova, N.S., Baturin, G.N., Gurvich, E.G., et al., 1987. Fe–Mn nodules and crusts from Japan Sea. Rep. Acad. Sci. USSR 293 (2), 430–434 (in Russian).
Severmann, S., Mills, R.A., Palmer, M.R., Fallick, A.E., 2004. The origin of clay minerals in active and relict hydrothermal deposits. Geochim. Cosmochim. Acta 68, 73–88.
Taira, A., 2001. Tectonic evolution of the Japanese island arc system. Annu. Rev. Earth Planet. Sci. 29, 109–134.
Tarakanov, R.Z., 1987. Seismicity Distribution of earthquake epicentres 1: 3 000 000 quantitiative characteristics of seismicity. In: Sergeyev, K.S., Krasny, M.L. (Eds.), Geology–Geophysical Atlas of the Kuril–Kamchatka Island System. Ministry of Geology of the USSR, Academy of Sciences of the USSR Ministry of Gas industry of the USSR, Leningrad. Sheet 33 (in Russian and English).
Taran, Yu.A., Pilipenko, V.P., Rozhkov, A.M., Vakin, E.A., 1992. A geochemical model of fumaroles of the Mutnovsky volcano, Kamchatka, USSR. J. Volcanol. Geotherm. Res. 49, 269–283.
Taran, Yu.A., Hedenquist, J.W., Korzhinsky, M.A., Tkachenko, S.I., Shmulovich, K.I., 1995. Geochemistry of volcanic gases from Kudryavy volcano, Iturup, Kuril Islands. Geochim. Cosmochim. Acta 59, 1749–1761.
Tarasov, V.G., Propp, M.V., Propp, L.N., Zhirmunsky, A.V., Namsaraev, B.B., Gorlenko, V.M., Starynin, D.A., 1990. Shallow-water gasohydrothermal vents of Ushishir Volcano and the ecosystem of Kraternaya Bight (The Kurile Islands). Mar. Ecol. 11, 1–23.
Thompson, G., Mottl, M.J., Rona, P.A., 1985. Morphology, mineralogy and chemistry of hydrothermal deposits from the TAG area, 26°N, mid-Atlantic Ridge. Chem. Geol. 49, 243–257.
Tolstykh, M.L., Naumar, V.B., Kononkava, N.N., 1997. Three types of melt in the basaltic andesite from the Medvezh'ya caldera, Iturup, southern Kurile islands. Geochem. Int. 35, 339–345.
Torokhov, P.V., 1992. Sulphide mineralization in hydrothermal deposits of the Piip volcano (Bering Sea). Rep. Acad. Sci. 326 (6), 1060–1063 (in Russian).
Toth, J.R., 1980. Deposition of submarine crusts rich in manganese and iron. Geol. Soc. Amer. Bull. Part I 91, 44–55.
Tsvetkov, A.A., 1991. Magmatism of the westernmost (Komandorsky) segment of the Aleutian Island Arc. Tectonophysics 199, 289–317.
Usui, A., Glasby, G.P., 1998. Submarine hydrothermal manganese deposits in the Izu–Bonin–Mariana Arc: an overview. Isl. Arc 7, 422–431.
Usui, A., Iizasa, K., 2002. Northwestern Pacific marine minerals data base (http://www.aist.go.jp/RIODB/db058/index.html).
Usui, A., Someya, M., 1997. Distribution and composition of marine hydrogenetic and hydrothermal manganese deposits in the northwest Pacific. In: Nicholson, K., Hein, J.R., Bühn, B., Dasgupta, S. (Eds.), Geol. Soc. Spec. Publ., vol. 119, pp. 177–198.
von Huene, R., Scholl, D.W., 1991. Observations at convergent margins concerning sediment subduction, subduction erosion, and the growth of continental crust. Rev. Geophys. 29, 279–316.
Wahrenberger, C., Seward, T.M., Dietrich, V., 2002. Volatile trace-element transport in high-temperature gases from Kudriavy volcano (Iterup, Kurile Islands, Russia). In: Hellmann, R., Wood, S.D. (Eds.), Water–Rock Interactions, Ore Deposits, and Environmental Geochemistry. Geochem. Soc. Spec. Publ. No., vol. 7, pp. 307–327.
Wei, D., Seno, T., 1998. Determination of the Amurian plate motion. In: Flower, M.F.J., Chung, S.-L., Lo, C.-H., Lee, T.-Y. (Eds.), Mantle Dynamics and Plate Interactions in East Asia. AGU Geodynamics, vol. 27, pp. 246–337.
Wright, I.C., de Ronde, C.E.J., Faure, K., Gamble, J.A., 2001. Discovery of hydrothermal mineralization from southern Kermadec arc volcanoes (SW Pacific). Earth Planet. Sci. Lett. 164, 335–343.
Zhuravlev, D.Z., Tsvetkov, A.A., Zhuravlev, A.Z., Gladkov, N.G., Chernyshev, I.V., 1987. $^{143}Nd/^{144}Nd$ and $^{87}Sr/^{86}Sr$ ratios in recent magmatic rocks of the Kurile island arc. Chem. Geol. 66, 227–243.